

PAPER

## Reducing MRI RF-induced heating for the external fixation using capacitive structures

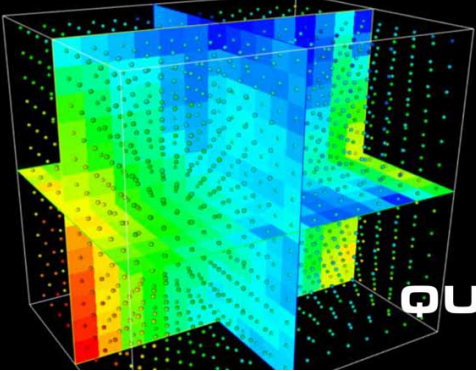
To cite this article: Jianfeng Zheng *et al* 2020 *Phys. Med. Biol.* **65** 155017

View the [article online](#) for updates and enhancements.

**GAMMA KNIFE®**  
Image Distortion Analysis  
with the **QUASAR™ GRID<sup>3D</sup>**

**WEBINAR** 

February 17, 2021 - 10 a.m. (EST)



**QUASAR** GRID<sup>3D</sup>  
BY MODUSQA



## PAPER

**RECEIVED**  
7 February 2020**REVISED**  
11 May 2020**ACCEPTED FOR PUBLICATION**  
27 May 2020**PUBLISHED**  
30 July 2020

# Reducing MRI RF-induced heating for the external fixation using capacitive structures

Jianfeng Zheng<sup>1</sup>, Rui Yang<sup>1</sup> , Qingyan Wang<sup>1</sup>, Ran Guo<sup>1</sup>, Jian Xu<sup>2</sup>, Xingxian Shou<sup>2</sup>, Wolfgang Kainz<sup>3</sup> and Ji Chen<sup>1</sup> 

<sup>1</sup> Dept. of Electrical and Computer Engineering, University of Houston, Houston, TX, 77204-4005, United States of America

<sup>2</sup> UIH America, Inc, Houston, TX 77054, United States of America

<sup>3</sup> Division of Biomedical Physics, Office of Science and Engineering Laboratories, Center for Devices and Radiological Health, U.S. FDA, Silver Spring, MD, 20993, United States of America

E-mail: [jchen18@uh.edu](mailto:jchen18@uh.edu)

**Keywords:** RF-induced heating, magnetic resonance imaging, external fixation device, insulating material

## Abstract

This paper presents a generic method to reduce the radiofrequency (RF) induced heating of external fixation devices during the magnetic resonance imaging (MRI) procedure. A simplified equivalent circuit model was developed to illustrate the interaction between the external fixation device and the MRI RF field. Carefully designed mechanical structures, which utilize capacitive reactance from the circuit model, were applied to the external fixation device to mitigate the coupling between the external fixation device and the MRI RF field for RF-induced heating reduction. Both numerical and experimental studies were performed to demonstrate the validity of the circuit model and the effectiveness of the proposed method. By adding capacitive structures in both the clamp-pin and rod-clamp joints, the peak specific absorption rate averaged in 1 gram (SAR<sub>1g</sub>) near the pin tips were reduced from 760.4 W kg<sup>-1</sup> to 12.0 W kg<sup>-1</sup> at 1.5 T and 391.5 W kg<sup>-1</sup> to 25.2 W kg<sup>-1</sup> at 3 T from numerical simulations. Experimental results showed that RF-induced heating was reduced from 7.85 °C to 1.01 °C at 1.5 T and from 16.70 °C to 0.32 °C at 3 T for the external fixation device studied here. The carefully designed capacitive structures can be used to detune the coupling between the external fixation device and the MRI fields to reduce the RF-induced heating in the human body for both 1.5 T and 3 T MRI systems. However, as RF-induced heating is very device and design specific all devices must be thoroughly tested based on its final design.

## 1. Introduction

Magnetic resonance imaging (MRI) has been a standard medical diagnostic tool over recent decades owing to its high-resolution imaging quality for soft tissue. Compared with x-ray or computed tomography (CT) imaging, MRI does not have ionizing radiation and long-term health risks (Shellock and Crues 2004). It is considered as one of the safest imaging methods in hospitals. However, patients with medical implants are usually restricted from MRI because of the potential safety concerns, especially the radiofrequency (RF) induced heating issue (Shellock *et al* 2009, Erhardt *et al* 2018). During the MR scan, the RF coil in the MRI machine will generate a strong RF field. As the RF field penetrates into the human body and interacts with the human tissue, a heating effect will occur. Particularly, the heating effect can become severe when the patients undergoing MRI have metallic devices implanted (Mohsin *et al* 2008, Zeng *et al* 2018). For example, the temperature rise of a deep brain stimulator under MRI can be as high as 25.3 °C (Rezai *et al* 2002). In addition to the fully implanted devices (Baker *et al* 2006, Calcagnini *et al* 2008), the external fixation device is another type of medical implants that can cause a severe heating concern (Luechinger *et al* 2006).

The external fixation device is a surgical device used to stabilize the fractured bones. A typical external fixation device consists of three parts: (1) metallic pins to be screwed into the fractured bones, (2) rods or bars made of carbon fiber or metallic materials to bridge the pins, and (3) metallic clamps to connect the

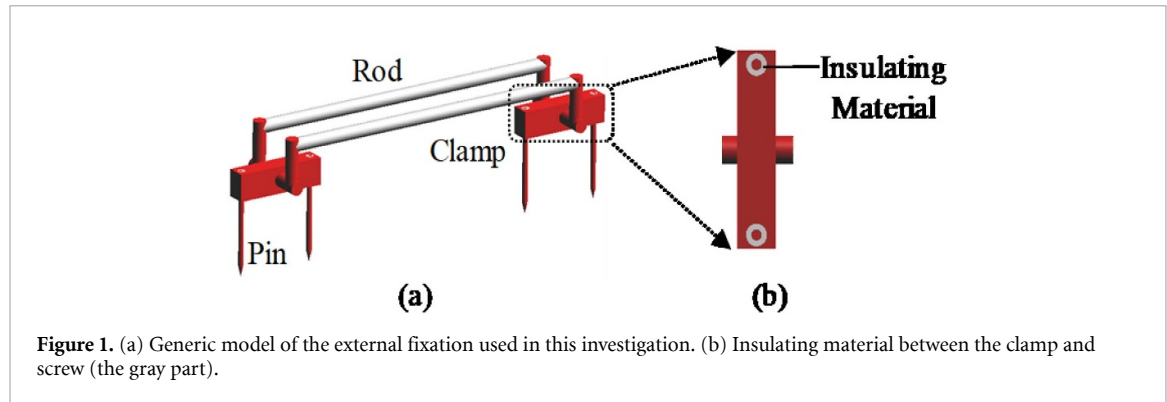


**Figure 1.** (a) Generic model of the external fixation used in this investigation. (b) Insulating material between the clamp and screw (the gray part).

pins and the rods. Comparing with other passive implants, the rods and clamps are outside the human body thus are much closer to the RF coils. It was observed that the external fixation device often leads to a higher heating effect than that of fully implanted passive devices (Liu *et al* 2012, 2013). Y. Liu *et. al.* investigated the RF-induced heating of generic external fixation devices and considered the impacts of the dimensions and configurations of the devices on the RF-induced heating (Liu *et al* 2012). It was shown that the external fixation device can cause a high local peak specific absorption rate over 1 gram (SAR<sub>1g</sub>) of around 800 W kg<sup>-1</sup> of and led to a temperature rise of more than 50 °C, in the specific settings.

To mitigate the RF-induced heating of the external fixations, Liu *et al* proposed to use insulating material to block the transmission of the RF energy to the pin tips (Liu *et al* 2014). They showed that applying proper insulating material, the RF-induced heating could be reduced by 67% at 1.5 T. Huang *et al* improved this method by changing the insulating material to absorbing material (Huang *et al* 2015). This material could further absorb part of the RF-induced energy received by the device frame, therefore reducing the heating effect in the human body. Although previous studies achieved good results in mitigating the RF heating of the external fixation, there are some limitations associated with these works. First, their studies only investigated the effects of the relative permittivity on the RF heating and failed to consider the effects of other parameters such as the thickness of the insulating material. Second, their methods were demonstrated at 1.5 T MRI. As high field MRI is widely used in clinical, there arises a need to investigate the effectiveness of the insulating/absorbing material in reducing RF heating of the external fixation devices at 3 T MRI. Moreover, it is essential to investigate the fundamental mechanism on how insulating/absorbing material can reduce RF-induced heating of the external fixation, and to develop a common method which can reduce the RF heating for various devices at both 1.5 T and 3 T.

In this paper, the effects of the insulating material on external fixation devices at 3 T MRI are investigated. While applying a thin insulating layer with low dielectric constant around the pins can reduce the RF-induced heating of the external fixation in 1.5 T MRI, the direct application of this method led to increased heating at 3 T MRI. To clarify the heating mechanism of the external fixation device and develop a general heating reduction method, an equivalent circuit model was developed. It shows that the most critical factor for heating reduction is to detune/mitigate the coupling between the external fixation devices and the RF fields from MRI systems. Carefully designed capacitive structures were then developed to investigate this strategy. Numerical simulations were performed to verify the validity of the circuit model and the proposed method to reduce the RF-induced heating of the external fixation device. Further experiments were conducted to demonstrate the effectiveness of the proposed method in reducing RF-induced heating for external fixation devices at 1.5 T and 3 T.

## 2. Materials and methods

### 2.1. External fixation device and its equivalent circuit

A generic tibia external fixation model was developed as shown in figure 1. It consists of three parts: (1) two metallic blocks to represent the clamps, (2) two straight rods to connect the clamps, and (3) four pins to be inserted into the human body. The clamp block has dimensions of 70 mm × 15 mm × 20 mm. The connecting rod has a diameter of 10 mm and a length of 250 mm. The pin has a diameter of 4 mm and a length of 78 mm, with an insertion depth of 2 cm from the surface of the phantom. These dimensional parameters are obtained from a commercial external fixation device. Compared with the real external fixation device, our designed model ignores some structural details, such as the threads on the screw tip. This is acceptable because the wavelength of the RF field in MRI is much larger than the screw thread. Using the simplified external fixation model can speed up the convergence time of the electromagnetic simulation.

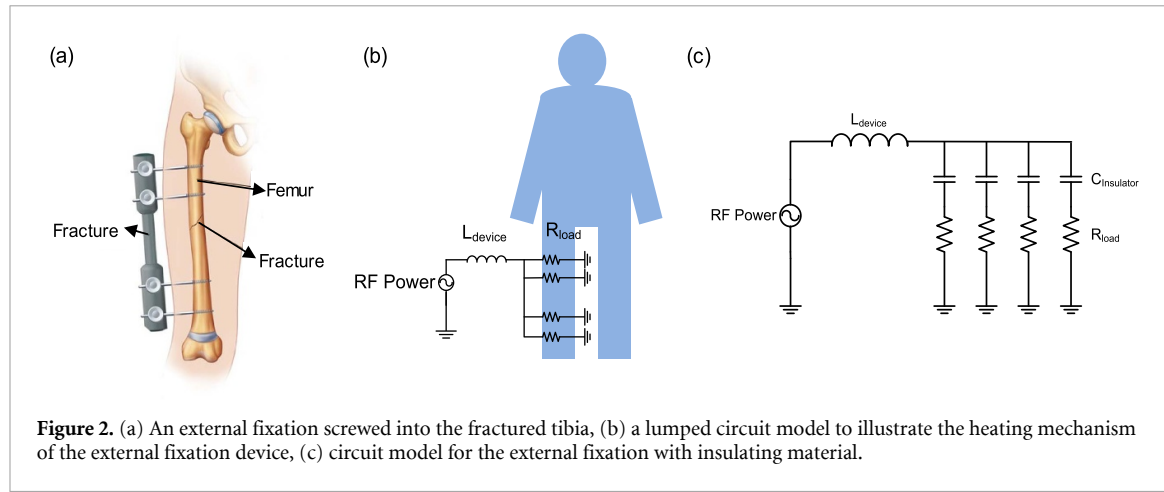


**Figure 2.** (a) An external fixation screwed into the fractured tibia, (b) a lumped circuit model to illustrate the heating mechanism of the external fixation device, (c) circuit model for the external fixation with insulating material.

To illustrate the heating mechanism of the external fixation device under the MRI RF exposure (Golestanirad *et al* 2019), an equivalent circuit was built as shown in figure 2. The RF power coupled to the external fixation device is modeled as a voltage source, which is mainly determined by the dimensions of the device (Acikel *et al* 2015, Missoffe *et al* 2018). The metallic device is modeled as an inductor due to the low conductive loss for this kind of device (Bottomley *et al* 2010). Since the human body dissipates the most induced-RF energy, four resistors are used to represent the tissues surrounding the four pins. The four resistors are connected in parallel, according to the structure of the external fixation device.

Based on the circuit theory, the dissipated power near the pin tips can be calculated as

$$P = I^2 R_{load} \quad (1)$$

where  $I$  is the induced current on the external device and is evaluated by

$$I = \frac{V_{RF}}{j\omega L_{device} + R_{load}}. \quad (2)$$

and  $R_{load}$  is the equivalent resistance of the four resistors.

If the total impedance of the equivalent circuit is increased, the induced current on the external fixation as well as the dissipated power near the pin tips will decrease. In other words, any structures that add extra resistance, capacitive reactance or inductive reactance, or a combination of these impedances to the circuit can reduce the RF-induced heating of the external fixations. Compare to other options, the capacitive structure is easier to implement, and has a less mechanical impact on external fixation devices. Therefore, a capacitive structure is used in this study.

A typical way to introduce capacitive impedance is to place an insulating material between two adjacent metallic faces. If the insulating material is lossy, it will introduce complex impedances including resistance and capacitive reactance. In this study, the insulating material is used as an example. After inserting insulation material between the joints of pins and clamps, the circuit model is modified as shown in figure 2(c). The equation to calculate the induced current on the device is then revised as

$$I = \frac{V_{RF}}{j\omega L_{device} + \frac{1}{j\omega C_{insulating\ cover}} + R_{load}}. \quad (3)$$

The capacitance of a cylindrical capacitor is calculated by

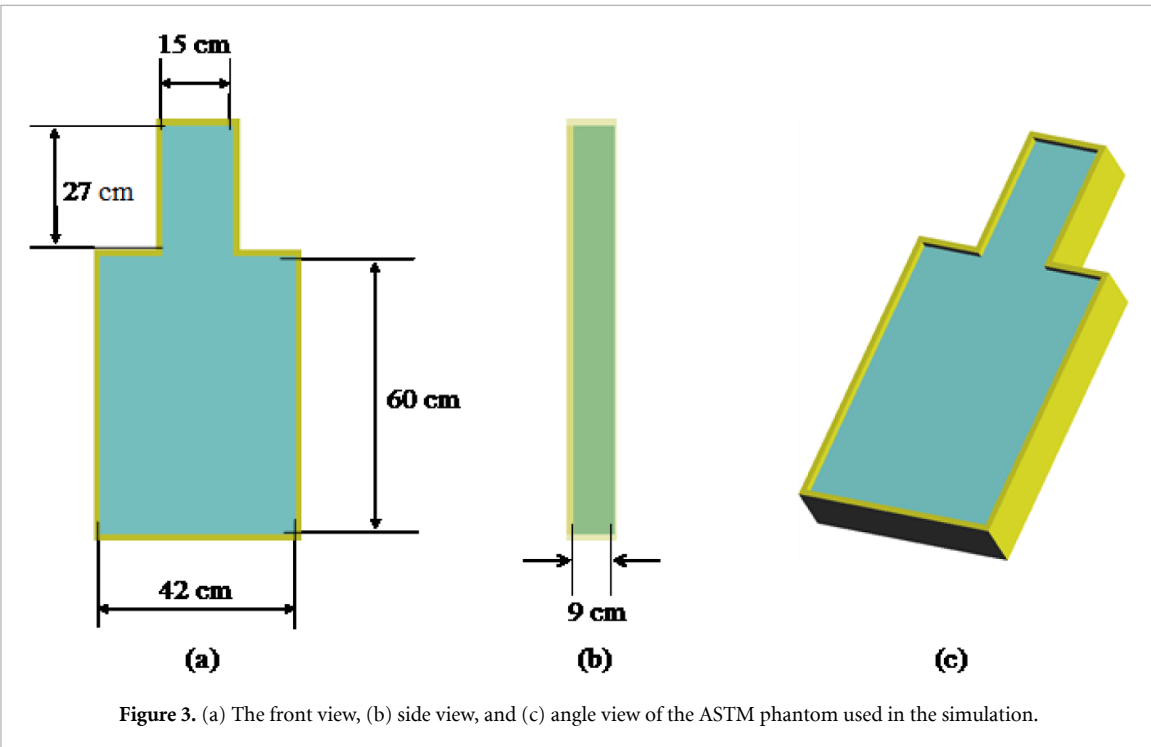
$$C = \frac{2\pi\epsilon_0\epsilon_r h}{\ln(b/a)} \quad (4)$$

where  $a$ ,  $b$  and  $h$  are the inner radius, outer radius, and height of the medium,  $\epsilon_r$  is the relative permittivity of the material.

The sum of the inductive reactance produced by the device and the capacitive reactance induced by the insulating material is defined as the total impedance of the device. According to the modified circuit model, if the total impedance of the device is increased, the induced current flowing to the human body will be decreased. As a result, less RF power will be dissipated near the pin tip and the heating effect is mitigated as well.

**Table 1.** Electrical properties for material at 128 MHZ.

	Relative Permittivity	Electrical Conductivity ( $\text{S m}^{-1}$ )
Phantom Gel	80.38	0.47
Phantom Shell	3.7	0
External Fixation	PEC	PEC
Insulating Material	2 ~ 9	0

**Figure 3.** (a) The front view, (b) side view, and (c) angle view of the ASTM phantom used in the simulation.

## 2.2. Numerical simulations

All the electromagnetic simulations were performed using the full-wave electromagnetic simulation software SEMCAD X (V14.8, SPEAG, Zurich, Switzerland). To generate the RF fields in the MRI system, high-pass birdcage coils were designed. Both coils have a diameter of 63 cm and a height of 65 cm. The eight parallel red lines represent the phased current sources and the sixteen blue lines at end rings are the tuning capacitors. The capacitors were adjusted to make the coil resonant at 64/128 MHz, which corresponds to the Larmor frequency of 1.5/3 T MRI system. Quadrature mode was used to excite the RF coils.

To evaluate the RF-induced heating near the medical implants under testing, the American Society for Testing and Material (ASTM) suggests a standard test method in F2182-11a (Anon 2013). According to the standard, a phantom material that simulates the electrical properties of the human body should be used. The dimensions of the phantom are shown in figure 3. The filled gel has a relative permittivity of 80.38 and a conductivity of  $0.47 \text{ S m}^{-1}$ . The shell of the phantom has a relative permittivity of 3.7 and a conductivity of zero. Besides, the implant to be tested should be placed where the incident field is strong. In this study, the external fixation model was placed 2 cm away from the inner sidewall of the ASTM phantom as shown in figure 3(c). The electrical properties for all materials used in this study are summarized in table 1.

In the post-process, the input power was set to achieve a whole-body averaged specific absorption rate (SAR) of  $2 \text{ W kg}^{-1}$  and 1-gram averaged  $\text{SAR}_{1g}$  near the pin regions were calculated for further analysis. The mesh step is 10 mm for the phantom shell and 5 mm for the gel. For the external fixation device, the maximum mesh step of 1 mm is used for the pins and the maximum mesh step of 2 mm is used for the rods and clamps. The numbers of the voxels are around 10 million for all simulations. A preliminary convergence study was performed to investigate the simulation time. It was shown that a simulation time of 20 periods is a good balance point between the convergence and computational burdens. Besides, the convergence of each simulation was checked when the simulation was finished.

## 2.3. Experimental measurements

During experiments, the ASTM phantom with a commercially available external fixation device was tested as an example. As shown in figures 4(a) and (b), both 1.5 T and 3 T MRI RF coils were used in the experiments.

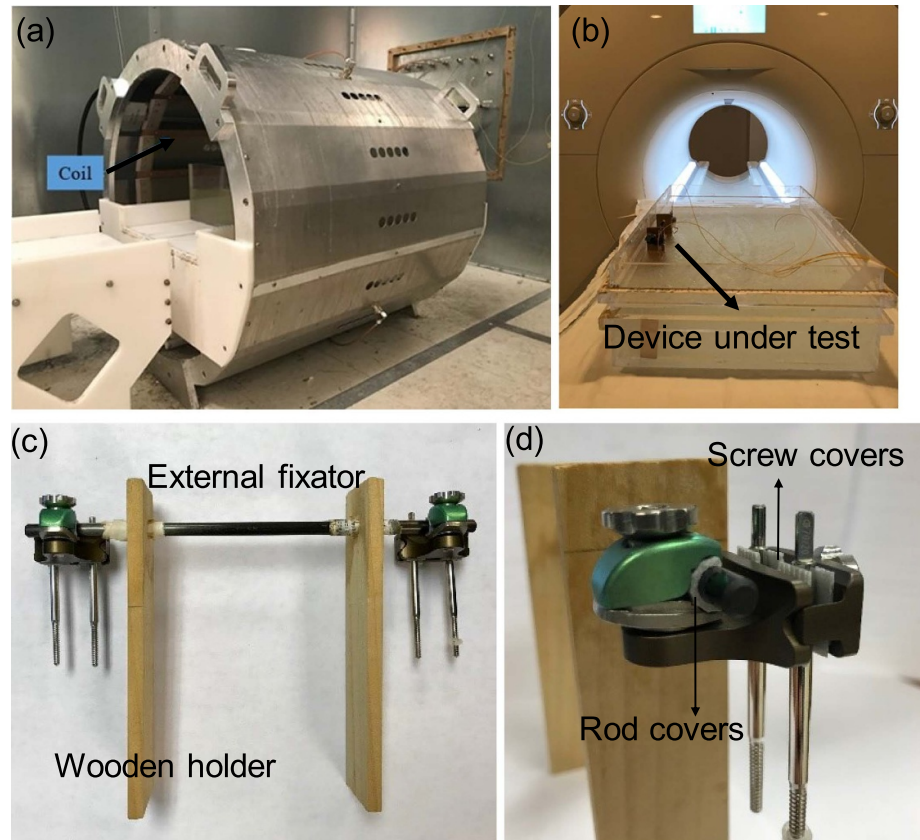


**Figure 4.** (a) A 1.5 T RF coil, (b) A 3 T MRI coil, (c) A commercial available external fixation device with wood holder, (d) insulating materials applied on the rods (rod covers) and pins (pin covers).

Optical-fiber thermal probes were used to measure the temperature rises near the pin tips. To hold the external fixation at the correct position, a wooden holder was used as shown in figure 4(c). Both rods and pins were covered with insulating layers as shown in figure 4(d). The insulating layer is made of polylactic acid (PLA), and its relative permittivity is about 3 (Dichtl *et al* 2017). The thickness of the rod cover is 2 mm and the thickness of the pin cover is 1 mm.

For the temperature measurements, we built the ASTM phantom with the following dimensions: 420 mm × 180 mm × 650 mm. The ASTM phantom was filled with GEL made of sodium chloride (NaCl, 1.32 g l<sup>-1</sup>) and polyacrylic acid (10 g l<sup>-1</sup>) dissolved in water. The phantom was filled with GEL to a depth of 90 mm. Based on the simulated results, the optical-fiber thermal probes were placed at the tips of the device pins. The total exposure time of the tested device in the RF field is 12 mins at 1.5 T and 6 mins at 3 T.

### 3. Results

Based on the numerical and experimental procedures described in the previous section, the results are presented here to demonstrate the validity of the circuit model and the effectiveness of the capacitive structures.

#### 3.1. Effect of relative permittivity

First, the effect of the relative permittivity of the insulating material on the RF-induced heating is studied. The insulating material was initially inserted between the pins and clamps and has a fixed thickness of 2 mm. Figure 5 shows the peak SAR<sub>1g</sub> values as a function of the relative permittivity of the insulating material. The peak SAR<sub>1g</sub> value for the external fixation without insulating material is also provided as a reference. It is found that decreasing the relative permittivity of the insulator will reduce the heating in 1.5 T MRI, which is consistent with previous studies. However, it will increase the heating in 3 T MRI. Figure 6 shows the simulated local SAR<sub>1g</sub> distributions for the external fixation devices without insulating material and with insulating material ( $\epsilon_r = 2$ ) at both 1.5 T and 3 T. In this figure, 0 dB corresponds to the peak SAR<sub>1g</sub> value of the external fixation without pin covers. For 1.5 T, the value is 752 W kg<sup>-1</sup>. For 3 T, this value is 388 W kg<sup>-1</sup>. As the relative permittivity of the insulating material goes 2, the peak SAR<sub>1g</sub> will decrease from 752 W kg<sup>-1</sup>

(without pin covers) to  $61 \text{ W kg}^{-1}$  at 1.5 T, while it will increase from  $388 \text{ W kg}^{-1}$  (without pin covers) to  $850 \text{ W kg}^{-1}$  at 3 T.

This fact can be illustrated by the circuit model in figure 2. At 1.5 T, the working frequency of the RF coil is 64 MHz. The inductive reactance generated by the device is insubstantial, which can be easily compensated by the capacitive reactance from the insulating covers. As the relative permittivity of the insulating material decreases, the capacitive reactance will increase, subsequently increasing the total impedance of the device and preventing the induced current from flowing into the load. Therefore, less power is dissipated by the gel and less heating is induced.

As the frequency is increased to 128 MHz at 3 T, the inherent inductive reactance of the device is increased and becomes significant. Increasing capacitive reactance will offset the inductive reactance, which eventually reduces the total impedance of the device. Therefore, a low dielectric constant that induces a large capacitive reactance will lead to higher RF-induced heating at 3 T MRI. The worst heating is generated when the device is in the resonance mode (Yeung *et al* 2002). As the added capacitive reactance exactly cancels the inductive reactance of the circuit, the induced current will reach the maximum value, causing severe heating near the pin tip.

### 3.2. Effect of the thickness

In this section, the effect of insulating layer thickness on the RF-induced heating is investigated and the result is shown in figure 7. At 1.5 MRI, the RF-induced heating is decreased as the thickness increases from 1 mm to 3 mm. This fact also can be explained by the circuit model. According to equation (4), the capacitance introduced by the insulating layer will decrease with the thickness of the insulating layer. Moreover, a smaller capacitance leads to a larger capacitive reactance, which prevents the RF-induced current from flowing into the lossy GEL. Therefore, less RF energy is concentrated near the pins of external fixation devices and the RF-induced heating is subsequently mitigated as well.

Compared with 1.5 T MRI, the RF-induced heating is not necessarily decreased at 3 T MRI by increasing the thickness of the insulating layer. It is observed that the worst-case of RF-induced heating values can occur with different material permittivity and insulating layer thickness combinations for 3 T MRI. This finding is consistent with the proposed circuit model. As analyzed above, the worst-case of heating happens when the added capacitive reactance exactly offsets the inductive reactance of the circuit. For a specific external fixation device, the capacitance value for the equivalent circuit at the resonant condition is a constant number. After increasing the thickness of the insulating layer, to obtain the same capacitance, the relative permittivity of the insulating material also increases. Therefore, the worst-case heating shifts towards a higher relative permittivity as the thickness of the insulating layer increases. When the thickness of the insulating material increases to 3 mm, the RF heating of the external fixation at 3 T can be mitigated to a peak local  $\text{SAR}_{1g}$  of  $64.53 \text{ W kg}^{-1}$  by applying an insulating layer with a relative permittivity of 2. This fact indicates that as long as the insulating material is sufficient thick, a low dielectric constant can still reduce the RF heating of the external fixation in 3 T MRI.

### 3.3. Adding more capacitive structures

According to the circuit model, increasing the total impedance of the device is the most critical factor to reduce the RF heating of the external fixation device. Due to the inherent inductance from the metallic device, the total impedance of the circuit is dependent on the difference between the capacitive reactance from the insulating material and the inherent inductive reactance. Therefore, we propose to add more capacitive structures to the external fixation device to minimize the RF-induced heating at 3 T MRI. The purpose of adding extra insulating layers is to introduce larger capacitive reactance in series so that the overall impedance is sufficiently large to prevent the induced current propagating towards the pin tips after canceling the inherent inductive reactance. Specifically, extra insulating materials with a dielectric constant of 2 and a thickness of 2 mm were added in the joints of the rods and clamps in the simulations.

Figure 8 shows the peak  $\text{SAR}_{1g}$  of the external fixation with various rod lengths at 1.5 T and 3 T. The blue bars indicate the heating of the device without insulators, while the orange bars indicate the heating of the device with insulating covers around both pins and rods. At both 1.5 T and 3 T, adding extra capacitive structures in the rod-clamp joints can effectively reduce RF-induced heating. Moreover, it is found that the heating reduction effect works for external fixation devices with different rod lengths. For 1.5 T, the RF-induced heating can be reduced by 98.18% to 98.47%, with an averaged value of 98.35%. For 3 T, the heating can be reduced by 93.56% to 95.90%, with an averaged value of 95.24%. This result demonstrates that detuning the equivalent circuit and increasing the total impedance of the device can lead to reduced RF-induced heating for the external fixation devices.

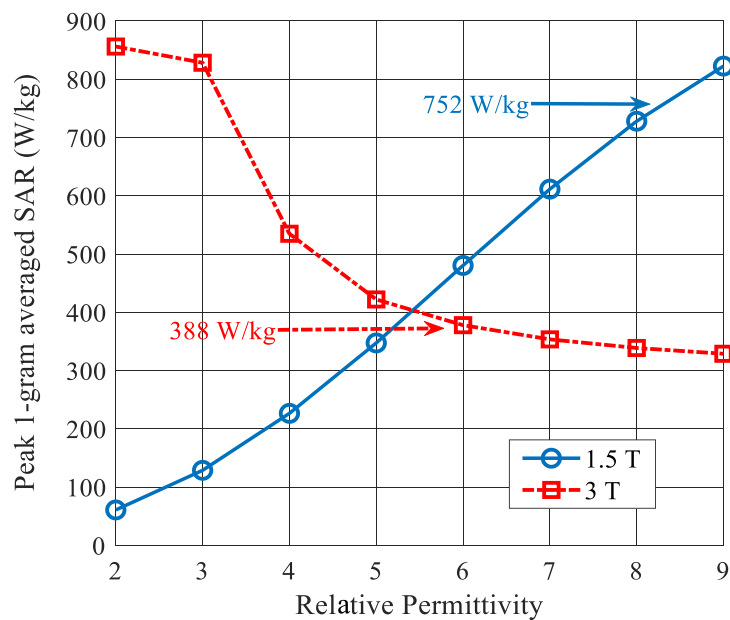


**Figure 5.** Simulated peak  $\text{SAR}_{1g}$  of external fixation varied with relative permittivity of the insulator at 1.5 T (blue solid line) and 3 T (red dash line). The blue and red arrows indicate the heating levels of external fixation without insulating material at 1.5 T and 3 T, respectively.

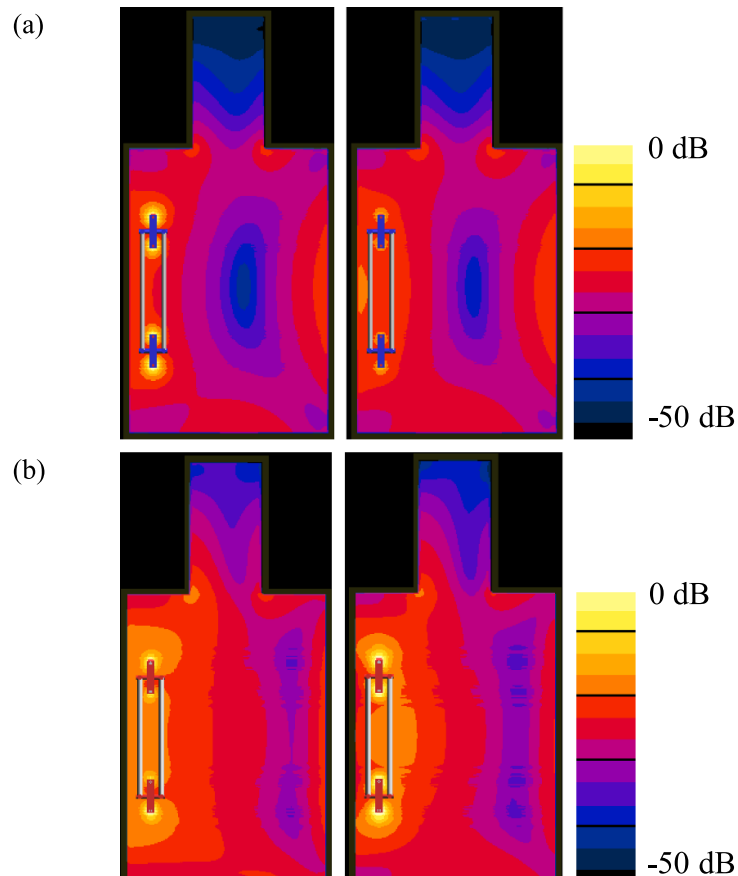


**Figure 6.** Simulated local  $\text{SAR}_{1g}$  distributions in the ASTM phantom with traditional external fixation device (left) and modified external fixation device (right) at (a) 1.5 T, and (b) 3 T. The modified external fixation device is inserted with 2-mm insulating layers ( $\epsilon_r = 2$ ) between the pins and clamps.

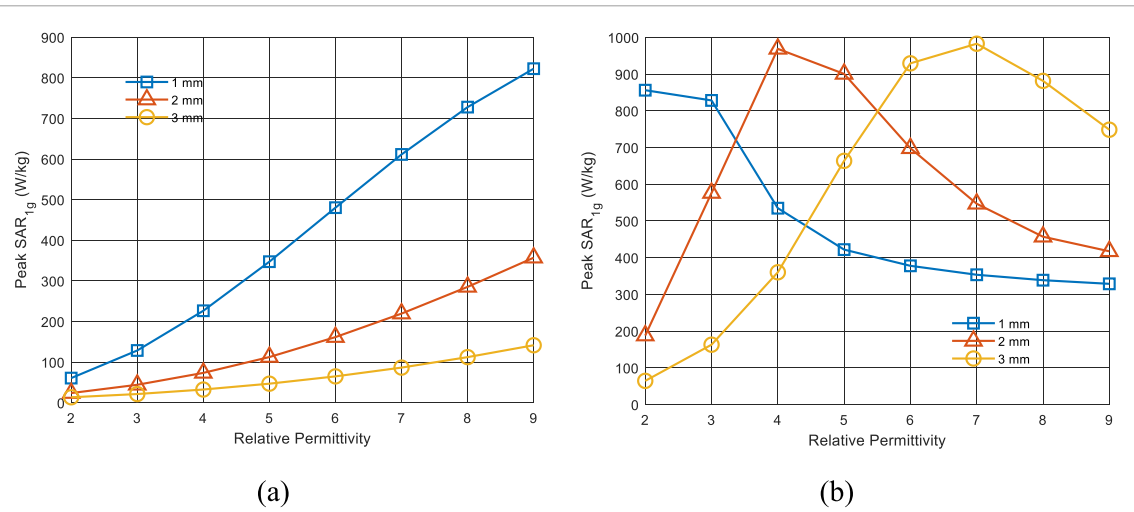


Figure 7. Simulated RF-induced heating varied with the thickness of the insulating layer at (a) 1.5 T MRI, (b) 3 T MRI.

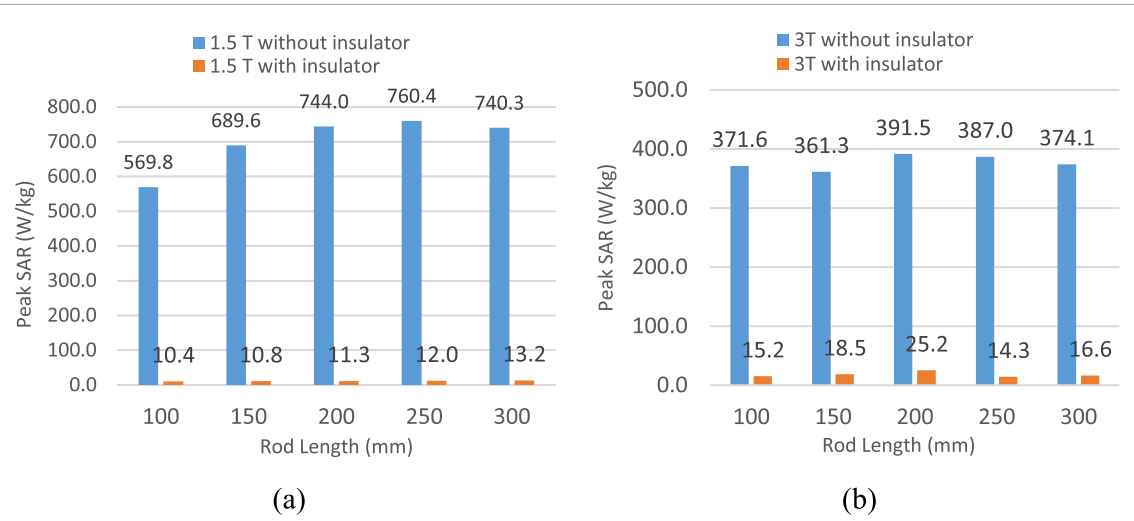


Figure 8. Simulated peak SAR<sub>1g</sub> of external fixation varied with rod length at 1.5 T and 3 T. The blues bars indicate the case without insulating covers, while the orange bars indicate the case with insulating covers on both rods and pins.

### 3.4. Experimental validation

To validate the effectiveness of the detuning strategy in a real clinical scenario, heating measurements were performed for the external fixation device with and without insulating covers in both 1.5 T and 3 T MRI coils. A commercially available tibia external fixator was used for testing through the experiments. A thicker insulating layer of 3 mm was not used since it would lead to mechanical instability of the construct.

Figure 9(a) shows the temperature rises of the external fixators with and without insulating covers at 1.5 T. It is obvious that the temperature rises of the external fixation device are significantly reduced through applying insulating covers around the rods and pins. The temperature rise for the device without insulating covers is 7.85 °C, while it is only 1.01 °C for the device with insulating covers. A heating reduction of 87.13% is achieved by placing insulating materials in both clamp-rods joints and clamp-pin joints. The same effect is observed at 3 T. It is shown in figure 9(b) that the temperature rise is reduced from 16.70 °C to 0.32 °C at 3 T. A heating reduction of 98.08% is achieved. Experimental results demonstrate that the proposed detuning method can reduce the heating of the external fixations at both 1.5 T and 3 T MRI. Furthermore, it also verifies the validity of the circuit model for the external fixation system and indicates that increasing the total impedance of the external fixation is essential in reducing the heating effect in MRI.

## 4. Discussion

Recent investigations have shown that insulating materials have the potentials to reduce the RF-induced heating of external fixations. However, most studies focus on the effects of insulating materials at 1.5 T MRI

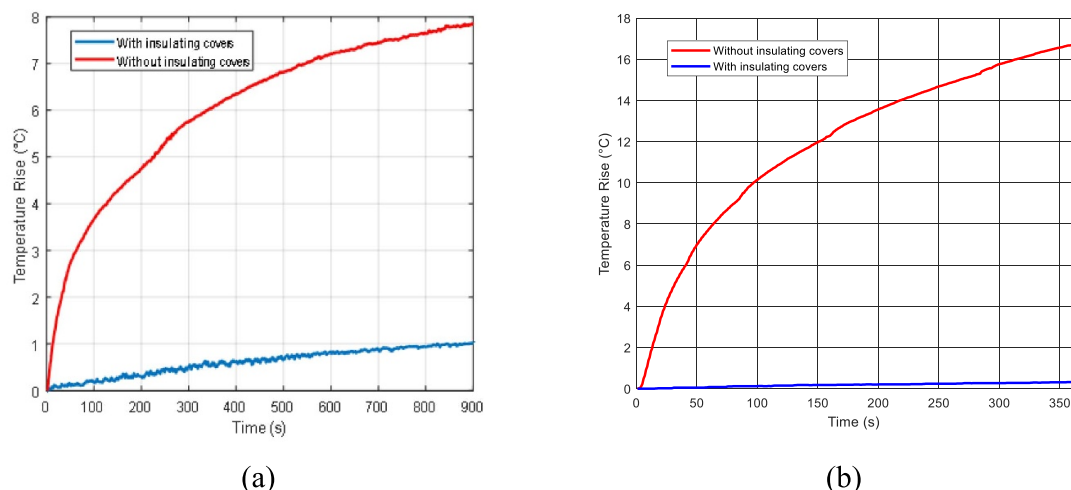


Figure 9. Measured temperature rise near the pin tip of the external fixation device with and without insulating covers.

rather than high field MRI. Moreover, the fundamental mechanism of the insulating materials in reducing the RF-induced heating fails to be illustrated completely and thoroughly. In this paper, we used the numerical and experimental methods to investigate the effectiveness of using insulating materials in reducing RF-induced heating at both 1.5 T and 3 T. It is found that inserting insulating material between the pins and clamps contact can effectively reduce the RF-induced heating for external fixations at 1.5 T. In addition, decreasing the dielectric constant and increasing the thickness of the insulating materials can further reduce the heating at 1.5 T. However, this method cannot mitigate the RF-induced heating at 3 T. In the specific case, placing insulating material with low relative permittivity in the clamp-pin joints will even aggravate the RF-induced heating at 3 T. This finding indicates that heuristically or intuitively applying pin covers is not guaranteed to reduce RF-induced heating of external fixation devices, carefully design procedure is needed to detune the coupling between the external fixation device and the RF field.

To explain the heating mechanism of the external fixations, we built an equivalent circuit model. According to the model, the external fixation device can be regarded as an RF voltage source connected with a lumped inductor. The effects of the power dissipation near the pin tip can be modeled as a resistive load. The RF-induced heating results from the RF power dissipated by the tissue. At 1.5 T, when we apply insulating covers with low relative permittivity on the pins, the overall impedance of the device will become capacitive. As the relative permittivity of the material decrease and the thickness of the covers increases, the capacitive impedance of the device will increase. Subsequently, the current flowing on the device is decreased. As a result, the dissipated power near the tip is reduced as well as the heating effect.

By comparison, at 3 T MRI, the external fixation device will resonant as the capacitive reactance introduced by the pin covers exactly cancels the inductive reactance of the device. The resonant condition of an RLC circuit is  $\omega^2 LC = 1$ . For a specific external fixation device, the inductance of the device is fixed. As the MRI frequency increases to 128 MHz at 3 T, the capacitance required to make the circuit resonant will decrease. Therefore, either reducing the relative permittivity of the insulating material or increasing its thickness will reduce the capacitance and cause the device resonant. Once the resonance occurs, the currents on the device and the dissipated power near the pin tips will reach maximum value. The worst-case heating then occurs.

To avoid the worst-case RF-induced heating and further reduce this heating, detuning the resonant circuit and increasing the equivalent impedance of the external fixation is necessary. In this study, introducing extra capacitive structures to the external fixation device was applied. By placing extra insulating materials in the joints of the rods and clamps, the equivalent circuit of the external fixation is detuned and the impedance of the device is increased. It is found from the simulated results that by placing insulating materials in both clamp-rod joints and clamp-pin joints, the RF-induced heating is reduced by 98.35% at 1.5 T and 95.24% at 3 T on average. Moreover, the experiments were performed to validate the simulations. Heating measurements show that the temperature rise near the pin tip is reduced from 7.85 °C to 1.01 °C for 1.5 T and 16.70 °C to 0.32 °C for 3 T. Both simulated results and experimental results demonstrate that detuning the equivalent circuit of the external fixation device and further increasing the device impedance effectively mitigate the RF-induced heating at both 1.5 T and 3 T.

It is worth noting that applying capacitive structures to external fixation devices may not eliminate the artifacts resulting from the metallic medical devices. Therefore, it is not straightforward to image the tissues near the external fixation device, even the device is modified with capacitive structures. However, the strategy of applying capacitive structures will still be helpful for patients with tibia external fixation devices who require torso or brain scans under MRI. This application enlarges the safety margin for patients with external fixation devices undergoing MRI.

## 5. Conclusion

In this paper, we proposed a promising method to reduce the RF-induced heating of the external fixation at both 1.5 T and 3 T MRI. An equivalent circuit was developed to shed light on the underlying mechanism of the heating effect for the external fixation device under the MR scan. It is concluded from the circuit model that increasing the equivalent impedance of the external fixation device can reduce the RF-induced heating for the external fixation system. Furthermore, it is found that the RF-induced heating will become extremely severe at 3 T MRI when the external fixation device simply has insulating material covered in the joints of the pins and the clamps. This is because that the capacitive reactance introduced by the pin covers exactly cancels the inherent inductive reactance of the device at 3 T. By applying insulating materials on both rods and pins, we successfully detuned the equivalent circuit of the external fixation and increased the total impedance of the device. Both simulated results and experimental results show that the RF-induced heating of the external fixation is reduced using this method. In future investigations, it is necessary to validate the effectiveness of the detuning strategy for various external fixation types and different MRI frequencies. However, the proposed method of using insulating materials on both rods and pins to reduce RF-induced heating is a device specific design. Simply adding insulating materials to existing devices does not guarantee MRI safety. Also, the safety of external fixation devices, or any other devices, using this method to reduce RF-induced heating cannot be assessed by leveraging existing RF-induced heating data from devices which do not use insulating materials. RF-induced heating and the proposed method is very device and design specific. Therefore, all devices must be thoroughly tested based on its final design.

## Disclaimer

The mention of commercial products, their sources, or their use in connection with material reported herein is not to be construed as either an actual or suggested endorsement of such products by the Department of Health and Human Services. The findings and conclusions in this article have not been formally disseminated by the Food and Drug Administration and should not be construed to represent any Agency determination or policy.

## ORCID iDs

Rui Yang  <https://orcid.org/0000-0002-7633-3253>  
Ji Chen  <https://orcid.org/0000-0001-6944-2729>

## References

Acikel V, Uslubas A and Atalar E 2015 Modeling of electrodes and implantable pulse generator cases for the analysis of implant tip heating under MR imaging *Med. Phys.* **42** 3922–31

Anon 2013 Standard Test Method for Measurement of Radio Frequency Induced Heating On or Near Passive Implants During Magnetic Resonance Imaging ASTM F2182-19e2 (<https://www.astm.org/Standards/F2182.htm>)

Baker K B, Tkach J A, Phillips M D and Rezai A R 2006 Variability in RF-induced heating of a deep brain stimulation implant across MR systems *J. Magn. Reson. Imaging* **24** 1236–42

Bottomley P A, Kumar A, Edelstein W A, Allen J M and Karmarkar P V 2010 Designing passive MRI-safe implantable conducting leads with electrodes *Med. Phys.* **37** 3828–43

Calcagnini G, Triventi M, Censi F, Mattei E, Bartolini P, Kainz W and Bassen H I 2008 In vitro investigation of pacemaker lead heating induced by magnetic resonance imaging: role of implant geometry *J. Magn. Reson. Imaging* **28** 879–86

Dichtl C, Sippel P and Krohns S 2017 Dielectric properties of 3D printed polylactic acid *Adv. Mater. Sci. Eng.* **2017** 6913835

Erhardt J B, Fuhrer E, Gruschke O G, Leupold J, Wapler M C, Hennig J, Stieglitz T and Korvink J G 2018 Should patients with brain implants undergo MRI? *J. Neural Eng.* **15** 041002

Golestanirad L, Angelone L M, Kirsch J, Downs S, Keil B, Bonmassar G and Wald L L 2019 Reducing RF-induced heating near implanted leads through high-dielectric capacitive bleeding of current (CBLOC) *IEEE Trans. Microw. Theory Tech.* **67** 1265–73

Huang X, Zheng J, Wu X, Kono M, Hozono H, Kainz W, Yang F and Chen J 2015 MRI heating reduction for external fixation devices using absorption material *IEEE Trans. Electromagn. Compat.* **57** 635–42

Liu Y, Chen J, Shellock F G and Kainz W 2013 Computational and experimental studies of an orthopedic implant: MRI-related heating at 1.5-T/64-MHz and 3-T/128-MHz *J. Magn. Reson. Imaging* **37** 491–7

Liu Y, Kainz W, Qian S, Wu W and Chen J 2014 Effect of insulating layer material on RF-induced heating for external fixation system in 1.5 T MRI system *Electromagn. Biol. Med.* **33** 223–7

Liu Y, Shen J, Kainz W, Qian S, Wu W and Chen J 2012 Computational study of external fixation devices surface heating in MRI RF environment *IEEE Int. Symp. Electromagn. Compat.* (Pittsburgh, PA) pp 612–6

Luechinger R, Boesiger P and Disegi JA 2006 Safety evaluation of large external fixation clamps and frames in a magnetic resonance environment *J. Biomed. Mater. Res. B Appl. Biomater.* **82** 17–22

Missoffe A, Kabil J, Vuissoz P A and Felblinger J 2018 Transmission line model of an implanted insulated cable for magnetic resonance imaging radiofrequency hazard evaluation *IEEE J. Electromagn. RF Microw. Med. Biol.* **2** 201–7

Mohsin S A, Sheikh N M and Saeed U 2008 MRI-induced heating of deep brain stimulation leads *Phys. Med. Biol.* **53** 5745–56

Rezai A R, Finelli D, Nyenhuis J A, Hrdlicka G, Tkach J, Sharan A, Rugieri P, Stypulkowski P H and Shellock F G 2002 Neurostimulation systems for deep brain stimulation: in vitro evaluation of magnetic resonance imaging-related heating at 1.5 Tesla *J. Magn. Reson. Imaging* **15** 241–50

Shellock F C and Crues J V 2004 MR procedures: biologic effects, safety, and patient care *Radiology* **232** 635–52

Shellock F G, Woods T O and Crues J V 2009 MR labeling information for implants and devices: explanation of terminology *Radiology* **253** 26–30

Yeung C J, Susil R C and Atalar E 2002 RF safety of wires in interventional MRI: using a safety index *Magn. Reson. Med.* **47** 187–93

Zeng Q, Wang Q, Zheng J, Kainz W and Chen J 2018 Evaluation of MRI RF electromagnetic field induced heating near leads of cochlear implants *Phys. Med. Biol.* **63** 135020